iScience

CellPress
OPEN ACCESS

Article

Uterine-specific *Ezh2* deletion enhances stromal cell senescence and impairs placentation, resulting in pregnancy loss

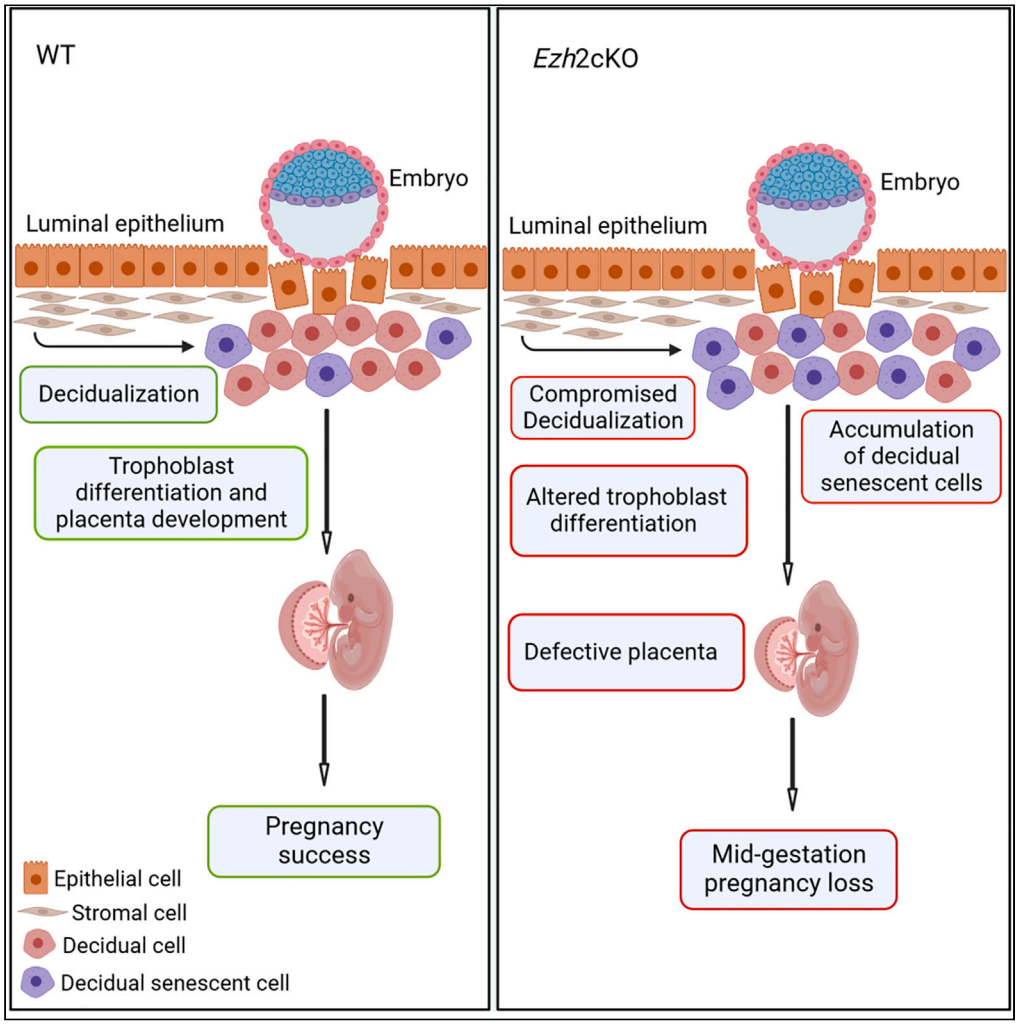

Vijay K. Sirohi, Theresa I. Medrano, Athilakshmi Kannan, Indrani C. Bagchi, Paul S. Cooke

ibagchi@illinois.edu (I.C.B.)
paulscooke@ufl.edu (P.S.C.)

Highlights

Loss of *Ezh2* results in mid-gestation pregnancy loss

EZH2 is necessary for decidualization and trophoblast differentiation

EZH2 regulates stromal cell senescence in decidua

*Ezh2*cKO mice exhibit placenta abnormalities

Sirohi et al., iScience 26, 107028
July 21, 2023
https://doi.org/10.1016/j.isci.2023.107028

iScience

CellPress
OPEN ACCESS

Article

Uterine-specific *Ezh2* deletion enhances stromal cell senescence and impairs placentation, resulting in pregnancy loss

Vijay K. Sirohi,[1] Theresa I. Medrano,[1] Athilakshmi Kannan,[2] Indrani C. Bagchi,[2,*] and Paul S. Cooke[1,3,*]

SUMMARY

Maternal uterine remodeling facilitates embryo implantation, stromal cell decidualization and placentation, and perturbation of these processes may cause pregnancy loss. Enhancer of zeste homolog 2 (EZH2) is a histone methyltransferase that epigenetically represses gene transcription; loss of uterine EZH2 affects endometrial physiology and induces infertility. We utilized a uterine *Ezh2* conditional knockout (cKO) mouse to determine EZH2's role in pregnancy progression. Despite normal fertilization and implantation, embryo resorption occurred mid-gestation in *Ezh2*cKO mice, accompanied by compromised decidualization and placentation. Western blot analysis revealed *Ezh2*-deficient stromal cells have reduced amounts of the histone methylation mark H3K27me3, causing upregulation of senescence markers p21 and p16 and indicating that enhanced stromal cell senescence likely impairs decidualization. Placentas from *Ezh2*cKO dams on gestation day (GD) 12 show architectural defects, including mislocalization of spongiotrophoblasts and reduced vascularization. In summary, uterine Ezh2 loss impairs decidualization, increases decidual senescence, and alters trophoblast differentiation, leading to pregnancy loss.

INTRODUCTION

Epigenetic regulation modulates gene expression in an organism without altering the DNA sequence and is responsible for transcriptional activation or suppression of genes to produce a unique pattern of a spatial-temporal gene activity. Enhancer of zeste homolog 2 (EZH2) is the rate-limiting catalytic subunit of the polycomb repressive complex 2 (PRC2), a histone methyltransferase critical for histone modifications that maintain gene repression.[1] PRC2 represses gene transcription by trimethylating histone 3 at lysine 27 (H3K27me3), which induces transcriptional silencing.[1] *Ezh2* overexpression or gain of function mutations occur in endometrial[2–4]; breast[5,6] and prostate[7] cancer, as well as in cancers of non-reproductive tissues.[8] Loss of function mutations in *Ezh2* are also associated with abnormal growth/cell proliferation.[8]

Some evidence suggests that EZH2 plays an important role in normal uterine physiology, as well as uterine pathologies such as endometrial cancer. We and others have reported that mice lacking uterine *Ezh2* are infertile by 8 months of age.[9,10] Uterine development was also affected and *Ezh2*cKO mice had increased numbers of uterine glands and age-dependent endometrial hyperplasia that led to organomegaly.[9,10] Moreover, in contrast to wild-type (WT) littermates, uterine epithelium of ovariectomized *Ezh2*cKO mice constitutively proliferates despite minimal circulating estrogen levels.[10–12] A luminal epithelial stratification and endometrial hyperplasia at later stages of uterine development has also been reported in *Ezh2*cKO mice.[9] Our recent study showed that uterine EZH2 loss is accompanied by high estrogen-independent expression of the protein kinase *p*-AKT,[13] but underlying molecular mechanisms responsible for aberrant epithelial proliferation and fertility defects in *Ezh2*cKO mice remain largely unknown.

Uterine preparation for pregnancy depends on an ordered progression of events involving uterine luminal and glandular epithelial proliferation followed by stromal cell proliferation and differentiation.[14,15] In mice, luminal and glandular epithelium proliferate rapidly at days 1 and 2 of pregnancy. As pregnancy proceeds, these cells exit the cell cycle and differentiate to become receptive for implantation. Implantation is initiated when the embryo attaches to the receptive uterine epithelium on day 4 of pregnancy. This is followed by invasion of the embryo into the underlying stroma and decidualization, the enlargement and

[1]Department of Physiological Sciences, University of Florida, Gainesville, FL, USA

[2]Department of Comparative Biosciences, University of Illinois at Urbana-Champaign, Urbana, IL, USA

[3]Lead contact

*Correspondence: ibagchi@illinois.edu (I.C.B.), paulscooke@ufl.edu (P.S.C.)

https://doi.org/10.1016/j.isci.2023.107028

differentiation of the fibroblastic stromal cells into secretory decidual cells, ensues.[16–18] A major function of decidual tissue is to protect the embryo and regulate its growth and development prior to placentation. The decidua secretes paracrine factors that promote angiogenesis, ensuring adequate oxygen and nutrient supplies to the embryo. Proper trophoblast differentiation is critical for normal placentation and is also influenced by secretion of unknown factors from differentiating stromal cells.[19,20]

Pregnancy loss or miscarriage is the most common pregnancy complication in the clinical setting,[21] and results from maternal uterine deficits, as well as fetal factors.[22,23] For example, decidualization facilitates embryo implantation and subsequent development,[16] and abnormal stromal cell decidualization is a major factor in recurrent miscarriages,[24] but the mechanism of this effect is poorly understood. Initial work indicated that down-regulation of EZH2 is critical for human uterine stromal cell decidualization.[25] In contrast, elevated EZH2 expression following embryo implantation in mouse decidual stromal cells suggests a potential role in the decidualization process.[26] However, the precise role and mechanisms of action of EZH2 in uterine decidualization remain unclear.

In this study, using genetic and cell biological approaches, we demonstrate that EZH2 regulates decidual senescence, trophoblast differentiation and placental development, and that uterine loss of EZH2 results in fetal resorption and pregnancy loss in mid-gestation. This study provides important insights into EZH2-mediated decidual function critical for placental development and establishment of pregnancy.

RESULTS

Uterine Ezh2 deletion results in mid-gestation pregnancy loss

We previously reported that *Ezh2* loss in uterus leads to infertility by 8 months of age.[10] To determine if normal fertilization/implantation occurred and the gestation stage at which *Ezh2* deficiency resulted in pregnancy loss, mice were sacrificed at GD7-15 of pregnancy. We observed comparable numbers of implantation chambers and indistinguishable size of implantation sites at GD7 in both genotypes (Figure 1A). By GD10, the implantation chamber size/diameter was significantly reduced ($p < 0.05$) with early signs of hemorrhage near the fetus (Figure 1B). Fetal growth restriction was apparent at GD12 and 15, when the fetal-placental unit was reduced by up to half ($p < 0.01$), with extensive hemorrhaging in *Ezh2*cKO compared to WT dams (Figures 1C and 1D).

We then analyzed fetal-placental units on GD15 to determine whether the defect occurs in the fetus and/or placenta. In contrast to WT females, *Ezh2*cKO dams lacked a recognizable placenta and fetus (Figure 1E). Since *Ezh2*cKO females are infertile at around 8 months of age, we determined the impact of *Ezh2* loss on the litter size of first pregnancy. Primiparous *Ezh2*cKO females had smaller litters compared to WT (Figure 1F). Collectively, these results indicated that *Ezh2*cKO dams showed embryo resorption and failed to carry pregnancy past mid-gestation, with extensive fetal hemorrhaging accompanying pregnancy loss.

Uterine Ezh2 deletion impairs decidualization and trophoblast differentiation

Although no apparent abnormality in gross morphology of implantation chambers was detected in pregnant *Ezh2*cKO dams at GD7, we observed distinct signs of embryo abnormalities upon analysis of uterine sections stained with hematoxylin and eosin (H&E) (Figure 2A). Since stromal cell proliferation, differentiation, decidual angiogenesis, and proper trophoblast differentiation are critical for establishment of pregnancy, we next analyzed these processes by immunofluorescent staining. We observed comparable stromal cell proliferation at GD7 in *Ezh2*cKO and WT mice, as shown by MKI67 staining (Figure 2B). Decidual angiogenesis as indicated by expression of an endothelial cell marker, CD31, was comparable in uterine sections of WT and *Ezh2*cKO mice on GD7 (Figure 2C). However, cytokeratin 8 immunostaining suggested altered trophoblast differentiation in *Ezh2*cKO dams in early pregnancy (Figure 2D). Since proper differentiation of the trophoblast cells is influenced by the decidual cells, we next examined decidualization in *Ezh2*cKO mice on GD7 using known biomarkers of decidualization, such as prolactin family 8, subfamily a, member 2 (*Prl8a2*), bone morphogenetic protein 2 (*Bmp2*), and homeobox A10 (*Hoxa10*) in GD7 uterine tissues. The mRNA expression for *Prl8a2* and *Bmp2*, but not *Hoxa10* in GD7 implantation sites was significantly decreased in *Ezh2*cKO compared to WT controls ($p < 0.05$) (Figure 2E).

In order to confirm that decidualization was suppressed in GD7 uteri, we utilized the oil-induced artificial decidualization model (Figure 3A). Control mice showed a robust decidual response 96 h after stimulation. In contrast, significant reductions in the weight of the stimulated uterine horn in *Ezh2*cKO mice suggested

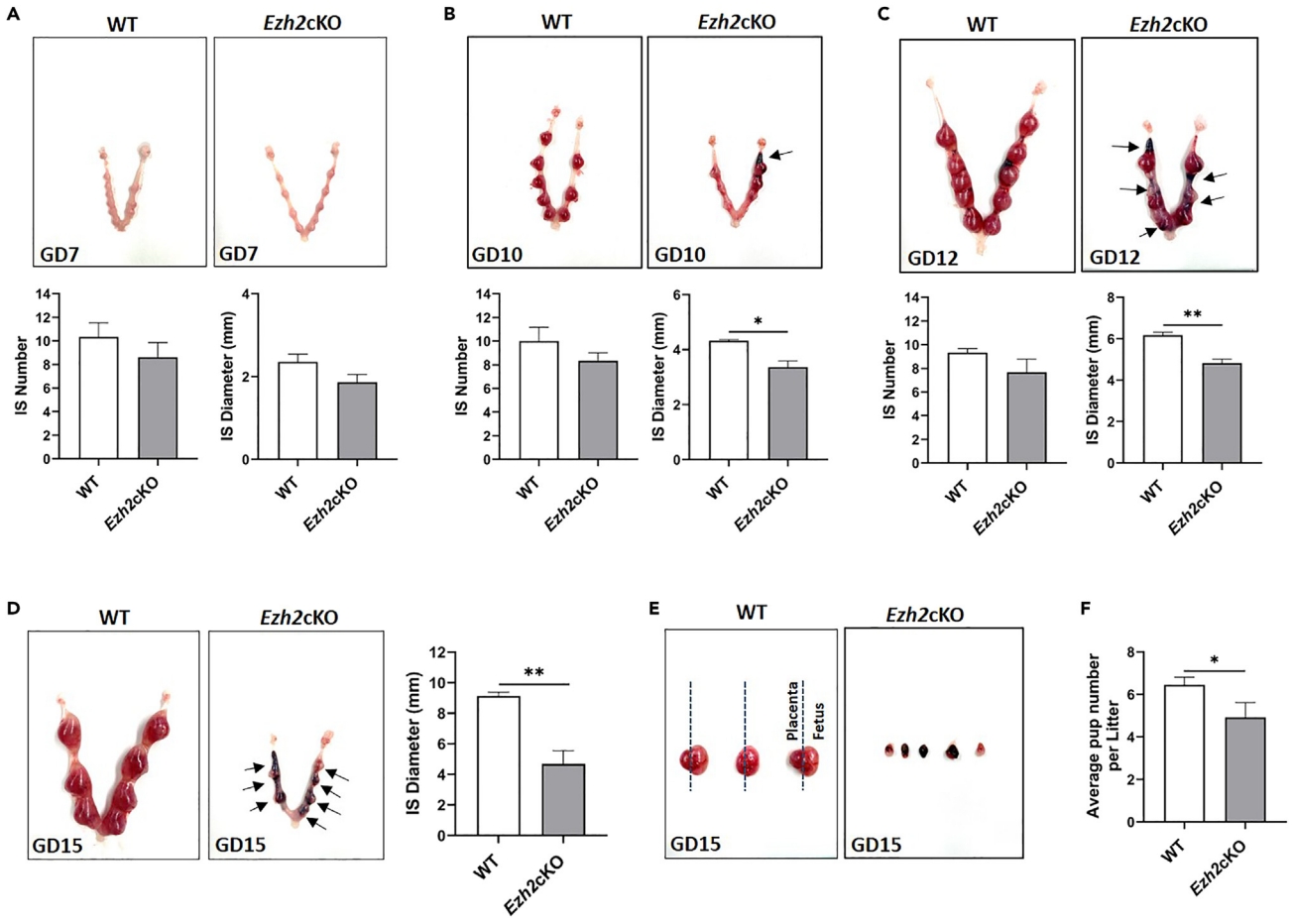

Figure 1. Mid-gestation pregnancy loss in *Ezh2*cKO mice

Upper panels: Embryo implantation sites in WT and *Ezh2*cKO uterine horns on (A) GD7, (B) GD10, and (C) GD12. Black arrowheads denote hemorrhagic sites. Implantation site (IS) number and diameter in WT and *Ezh2*cKO mice are shown in middle panels of Fig.1A (n = 5–8), B (n = 3) and C (n = 3–4). Lower panels: (D) Embryo implantation sites in WT and *Ezh2*cKO uterine horns on GD15 (left panel) and quantitation of implantation site diameter (right panel; n = 3). Black arrowheads show hemorrhagic sites and fetal resorptions in *Ezh2*cKO mice.

(E) At GD15, in contrast to WT, implantation sites in *Ezh2*cKO mice do not contain a recognizable placenta and fetus. All the images were captured at same magnification.

(F) Pup number in primiparous litters of WT and *Ezh2*cKO mice. n = 29 for WT, n = 12 for *Ezh2*cKO. Data are presented as mean ± SEM and were analyzed using the Student's *t* test. **p < 0.01 and *p < 0.05 vs. WT.

that *Ezh2* deletion reduced but did not completely abrogate decidualization ($p < 0.05$) (Figures 3B and 3C). Uteri in WT mice demonstrated fully differentiated stromal cells with characteristic large nuclei, while *Ezh2*cKO mice had a reduced response with less differentiated stromal cells (Figure 3D). However, stromal cell proliferation was comparable in both genotypes (Figure 3E). These findings revealed that uterine *Ezh2* deletion inhibited stromal decidualization, raising the possibility of subsequent placentation defects and intrauterine growth restriction of fetuses in *Ezh2*cKO dams.

Ezh2 deletion enhances stromal cell senescence and impairs decidualization

Since stromal cell differentiation but not proliferation was compromised in *Ezh2*cKO mice, we looked at stromal cell senescence, which has been reported to control decidualization and subsequent interaction with trophoblast cells.[27–29] Stromal cells isolated from WT and *Ezh2*cKO GD4 uteri were 95% pure as shown by positive immunohistochemical staining for the stromal marker vimentin and negative staining for the epithelial marker cytokeratin (data are not shown). Following 72 h of decidualization, stromal cells showed reduced expression of mRNA for the decidualization marker *Prl8a2*, consistent with our *in vivo* findings

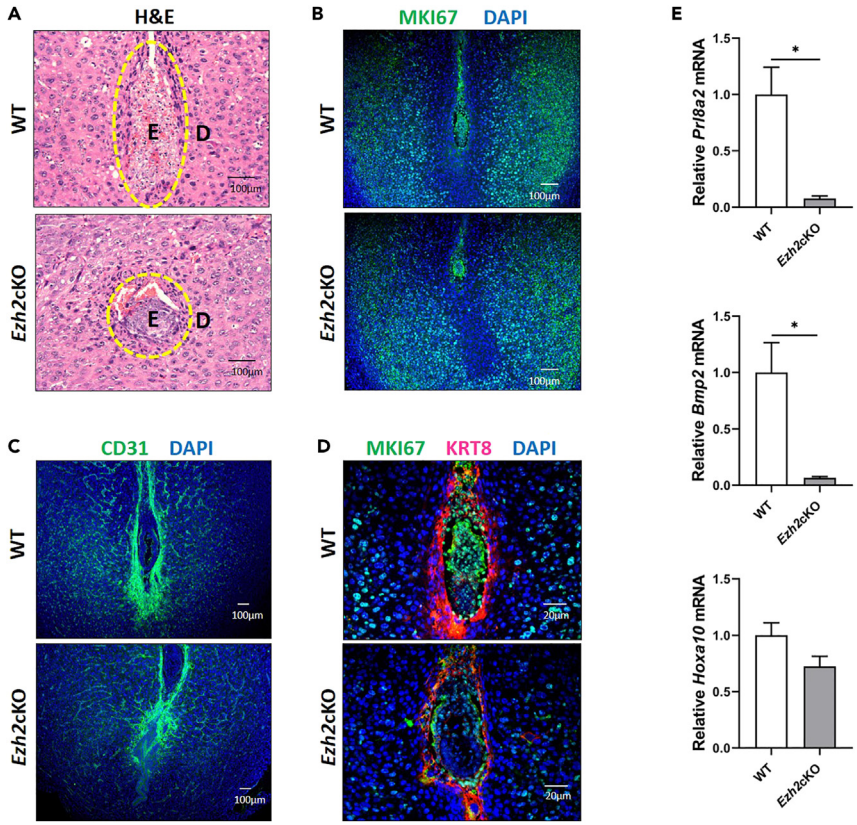

Figure 2. *Ezh2* loss impairs trophoblast differentiation and decidualization during early pregnancy

(A) GD7 implantation sites showing retarded growth in embryos (demarcated by dashed lines) from *Ezh2*cKO dams. E, embryo; D, decidua; magnification bars, 100μm.

(B) Immunofluorescence for MKI67 (green) in GD7 implantation sites. Nuclei were counterstained blue with DAPI. Magnification bars, 100μm.

(C) Decidual angiogenesis analysis using CD31 immunofluorescence in GD7 implantation sites from WT and *Ezh2*cKO mice. Magnification bars, 100μm.

(D) Immunofluorescence showing co-localization of trophoblast cell marker cytokeratin 8 (KRT8; red) and MKI67 (green) in GD7 implantation sites. Magnification bars, 20μm.

(E) mRNA levels of *Prl8a2*, *Bmp2* and *Hoxa10* in GD7 implantation sites from WT and *Ezh2*cKO mice. For comparisons, expression values were set to one in WT group. Data are presented as mean ± SEM and were analyzed by Student's *t* test, n = 3. Significant changes denoted by *$p < 0.05$ vs. WT.

($p < 0.01$) (Figure 4A). Stromal cells positive for senescence-associated β-galactosidase (SA-β-Gal) indicated enhanced senescence in stromal cells from *Ezh2*cKO mice ($p < 0.01$) (Figure 4B).

Cellular senescence is upregulated in Ezh2cKO uterine stroma

To confirm the increase in senescent stromal cells of *Ezh2*cKO uteri, we performed western blotting for the senescence markers p16 and p21. In *Ezh2*-deficient stromal cells, p16 and p21 expression was significantly upregulated ($p < 0.01$) (Figure 4C). Studies using the human decidualization model suggested that withdrawal of decidualization stimuli downregulates p53, but upregulates the phosphorylation and activation of AKT. In addition, *p*-AKT can also stabilize p21 to promote senescence. We detected suppressed p53 expression in *Ezh2*cKO stromal cells, whereas *p*-AKT levels were upregulated compared to WT controls ($p < 0.01$) (Figure 4C). Since histone methylation regulates DNA damage-independent senescence by upregulating p16 expression and EZH2 is the master regulator of histone methylation, we measured the H3K27me3 mark in stromal cells. H3K27me3 expression was strongly suppressed in *Ezh2*cKO stromal cells ($p < 0.01$), suggesting that *Ezh2* loss promotes senescence through p16 upregulation.

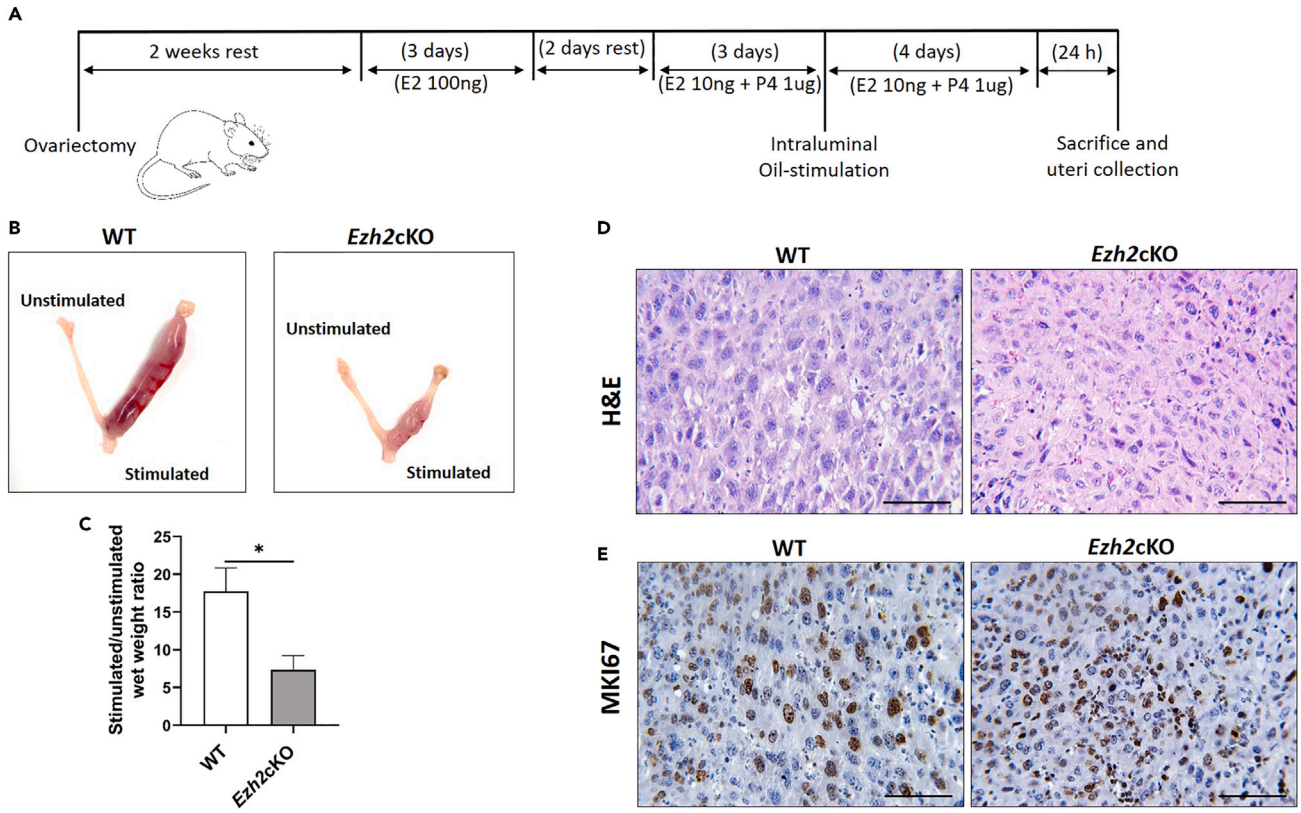

Figure 3. Decidualization is compromised in *Ezh2*cKO mice

(A) Artificial decidualization protocol.

(B) Gross morphology of unstimulated and oil-stimulated uterine horns from WT and *Ezh2*cKO mice after 5 days of oil stimulation.

(C) Ratio of uterine wet weight between oil-stimulated and unstimulated horns from WT (n = 3) and *Ezh2*cKO (n = 5) mice. Data are presented as mean ± SEM and were analyzed by Student's *t* test, *p < 0.05 vs. WT.

(D) H&E staining of unstimulated and oil-stimulated uterine horns of WT and *Ezh2*cKO mice. *Ezh2*cKO stromal cells have relatively smaller nuclei and less differentiated stroma, characteristics of altered decidualization.

(E) MKI67 immunohistochemistry in unstimulated and oil-stimulated uterine horns of WT and *Ezh2*cKO mice. Comparable expression of MKI67 was observed in WT and *Ezh2*cKO mice. Magnification bars, 100μm.

Loss of uterine Ezh2 impairs placental development

As pregnancy progress, trophoblast cells undergo a differentiation program to form placenta. To gauge the impact of uterine *Ezh2* loss on placental development, we investigated placental architecture at GD12. The WT GD12 placentas (Figure 5A) consisted of three well-organized layers: the labyrinth (L), the junctional zone (JZ) consisting of spongiotrophoblast and glycogen-rich trophoblast cells, and a layer of parietal trophoblast giant cells bordering the maternally derived decidua (D). However, placentas from *Ezh2*cKO mice exhibited various alterations in these placental layers. While some placentas were similar to WT, we observed a significantly smaller L layer and expanded JZ in some placentas from *Ezh2*cKO mice (Figure 5B).

To further investigate this abnormal placental morphology, placental samples from WT and *Ezh2*cKO were probed for trophoblast-specific protein alpha (TPBPA) using immunofluorescence. In WT mice, the TPBPA-positive spongiotrophoblast cells were localized exclusively in the JZ (Figure 5B). In contrast, in *Ezh2*cKO mice TPBPA immunostaining was significantly reduced in JZ spongiotrophoblast cells and aberrant infiltration of spongiotrophoblast cells occurred in the labyrinth layer (Figure 5B), indicating impaired placental development.

Trophoblast differentiation is essential for establishing cell lineages that regulate placental development, maintenance, and function. p57, a cyclin-dependent kinase (CDK) inhibitor, plays an important role in

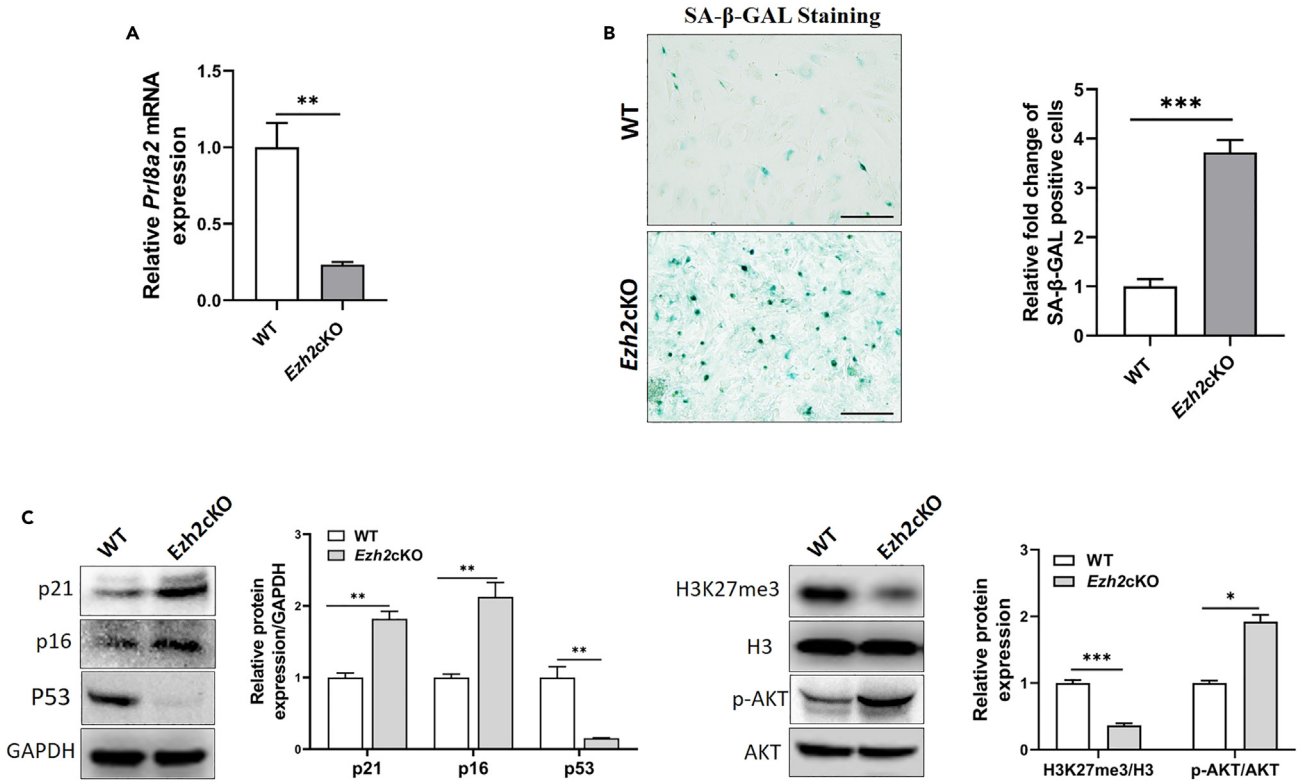

Figure 4. Increased stromal cell senescence in *Ezh2*-depleted stromal cells

(A) qRT-PCR analysis of *Prl8a2* expression. GD4 stromal cells from WT and *Ezh2*cKO pregnant mice were decidualized *in vitro* then harvested for RNA isolation and qRT-PCR. Data are presented as mean ± SEM; n = 3 for each genotype; magnification bars, 100μm.; **p < 0.01 vs. WT.

(B) SA-β-GAL staining in mouse primary stromal cells decidualized for 72h (left panel) and quantitation of SA-β-GAL-positive stromal cells (right panel).

(C) Western blots (left) showing p21, p16, p53, H3K27me3, and pAKT levels in WT and *Ezh2*cKO stromal cells decidualized for 72 h. Densitometric quantitation of protein expression levels are shown as fold change on the right. Data are presented as mean ± SEM and were analyzed using the Student's *t* test. **p < 0.01 vs. WT; n = 3 for each group.

development of labyrinth trophoblasts and spongiotrophoblasts in humans and mice.[30,31] To investigate whether trophoblast differentiation is affected in *Ezh2*cKO mice, we monitored p57 expression in GD12 placental samples. Placentas of WT mice abundantly expressed p57 in the JZ and labyrinth layer, but p57 was markedly reduced in *Ezh2*KO placentas (Figure 5B), indicating compromised trophoblast differentiation.

Decreased p57 expression in the labyrinth layer of *Ezh2*cKO placentas raised the possibility of impaired placental vasculature. Indeed, the WT placenta abundantly expresses the endothelial cell marker CD31 (Figure 5B), reflecting the widespread labyrinth vascular network. Labyrinth CD31 expression was severely attenuated in *Ezh2*cKO placentas, indicating defective vascularization (Figure 5B). Collectively, these results indicated that uterine *Ezh2* ablation interferes with trophoblast differentiation, causing defective placentation and fetal loss.

DISCUSSION

Miscarriage occurs in ~15% of clinically confirmed pregnancies and results in ~23 million pregnancy losses/year worldwide, and miscarriage rises with maternal age.[32,33] Although embryonic chromosomal abnormalities are a major cause of miscarriage, abnormalities in uterine structure and/or function are also associated with pregnancy loss.[33] Successful uterine remodeling immediately before and during early pregnancy are necessary to allow normal embryo implantation, stromal cell decidualization, trophoblast differentiation, and subsequent placental development required for normal pregnancy progression. Alterations of these processes at any stage may result in a loss of pregnancy.[16] Despite several uterine factors

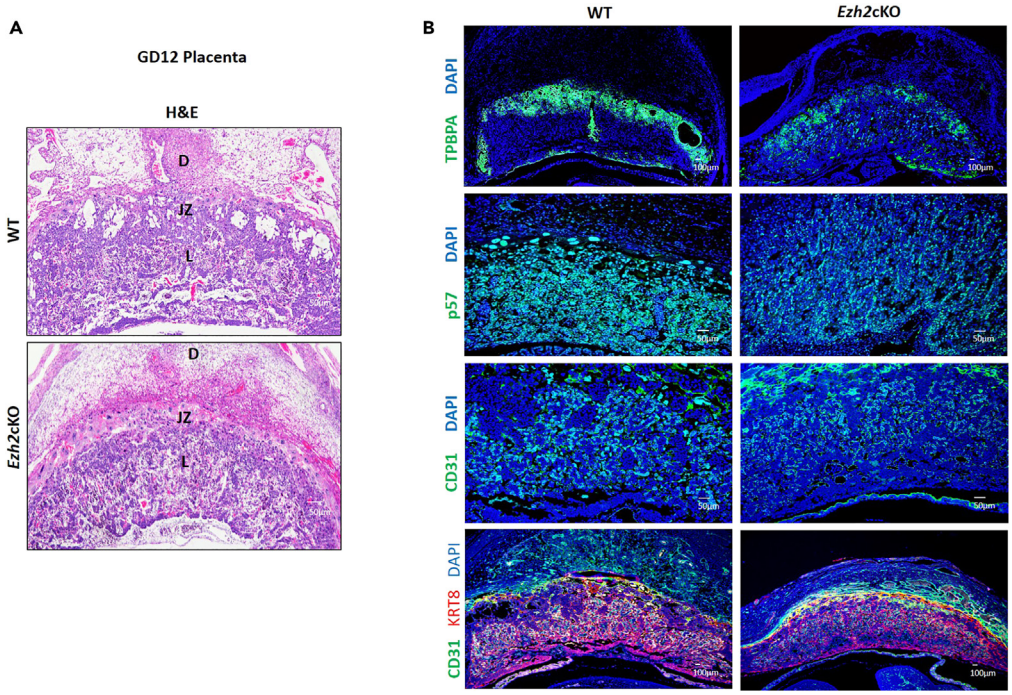

Figure 5. Placentation defects in *Ezh2*cKO mice

(A) Architectural defects in various layers of GD12 placenta from *Ezh2*cKO dams compared to WT. Labyrinth, L; Junctional zone, JZ; Decidua, D; magnification bars, 50μm.

(B) Immunofluorescence for placental proteins TPBPA, p57, CD31, and KRT8 in GD12 placenta from WT and *Ezh2*cKO dams. Nuclei were counterstained with DAPI. Reduced numbers of TPBPA-positive spongiotrophoblast cells are localized in the junctional zone, with aberrant infiltration in labyrinth layer of placenta from *Ezh2*cKO dams. In comparison to WT placenta, attenuated p57 expression occurs in both the junctional zone and labyrinth layer in placentas from Ezh2cKO dams. Suppressed CD31 expression indicates an altered vascular network in *Ezh2*cKO placenta. Co-localization of CD31 and KRT8 are also shown in yellow. n = 3; magnification bars, 50 and 100μm.

known to be associated with miscarriages, underlying molecular mechanisms by which a dysregulated uterine microenvironment induces miscarriage remain unclear.

The histomethyltransferase EZH2 can alter gene expression by trimethylating lysine-27 in histone 3 (H3K27me3) to repress gene transcription. EZH2 plays important roles in cell proliferation, apoptosis, and senescence in normal cells, and is also involved in neoplastic development and progression. Conditional uterine *Ezh2* deletion produces epithelial cell stratification and constitutive epithelial proliferation and alters uterine adenogenesis, resulting in infertility.[9,10,34] Despite defects in uterine development, *Ezh2*cKO mice become pregnant at 2–4 months. However, the pups per litter and pup survival were significantly reduced in *Ezh2*cKO dams at even 2 months of age.[10] Furthermore, *Ezh2*cKO mice exhibit normal ovarian functions, such as estrus cycle and the presence of normal numbers of corpora lutea, indicating normal ovarian function. This raises the possibility that uterine abnormalities in *Ezh2*cKO mice result in infertility.[10] The present study sought to determine the cause(s) of this infertility in *Ezh2*cKO mice.

Our findings indicated that *Ezh2* loss does not affect either fertilization or embryo implantation as indicated by the comparable number of implantation chambers in WT and *Ezh2*cKO mice. However, compared to WT mice, *Ezh2*cKO dams had reduced numbers of viable fetuses, suggesting pregnancy loss later in gestation. This accounts for the decreased primiparous litter size in *Ezh2*cKO mice, and the progressive infertility in these animals suggests that uterine dysfunctions affecting pregnancy outcome may be progressive with advancing age.

Stromal cell decidualization is necessary for pregnancy establishment as decidual cells supply nutrients and provide immune protection for the conceptus by suppressing maternal immune response. Decidualization defects are a major factor in recurrent pregnancy loss in women.[14,24,35] A recent study suggested that

Ezh2-deficient stromal cells show fibroblast activation and peri-embryonic collagen deposition, which leads to a wound healing response at the maternal-fetal interface, resulting in pregnancy loss.[36] Alterations in stromal cell proliferation and differentiation are hallmarks of defective decidualization in mice. PRL8A2 deficiency disrupts the pregnancy-associated uterine adaptations to hypoxia and results in pregnancy loss in mice.[37,38] In addition, BMP2 promotes differentiation through WNT4 activation in mouse and human endometrial stromal cells.[39] Although there was no significant change in stromal cell proliferation in GD7 uteri of *Ezh2*cKO mice, expression of classical decidualization markers such as *Prl8a2* and *Bmp2* were significantly reduced and their expression patterns were consistent with other previously used mouse models lacking uterine *Ezh2*.[9,34]

The artificial decidualization model is used to study *in vivo* decidualization in the absence of embryonic factors. The attenuated decidual response in *Ezh2*cKO mice following artificial decidualization further confirmed that observed decidualization defects result from altered uterine maternal factors, rather than from the embryo. Comparable stromal cell proliferation in WT and *Ezh2*cKO uteri suggested that altered cell multiplication does not account for impaired decidualization in *Ezh2*cKO uteri and that the compromised differentiation of stromal cells reflects intrinsic uterine factors rather than any fetal contribution.

Cellular senescence results in permanent cell-cycle arrest, but is not accompanied by cell death.[40] In recent years, enhanced decidual cell senescence has been reported to be associated with impaired decidualization and recurrent pregnancy loss.[27–29,41,42] Decidualization of stromal cells results in emergence of a large population of mature decidual cells and induces acute senescence in a subpopulation of stromal cells referred to as senescent decidual cells. Senescent decidual cells create a transient pro-inflammatory environment required for uterine remodeling to facilitate embryo implantation.[27] However, these senescent decidual cells must be eliminated after a short period of time by uterine natural killer (uNK) cells to return the uterine environment to normal.[43] In contrast, senescent decidual cells that persist in the uterus as chronic senescent cells can induce senescence in neighboring cells though paracrine signaling.[28,44] Accumulation of these chronic senescent cells leads to reduced uterine plasticity and impaired decidualization.

To better characterize factors involved in the impaired decidualization in *Ezh2*cKO mice, we utilized an *in vitro* model of this process. Reduced expression of the decidualization marker *Prl8a2* mRNA in *Ezh2*cKO decidual cells indicates abnormal decidualization *in vitro*. The increased senescent stromal cell population in *Ezh2*cKO uteri suggests that EZH2 normally inhibits decidual senescence. Interestingly, uNK cells and genes associated with their recruitment and differentiation appear to be significantly reduced in GD8 decidua in *Ezh2*cKO mice.[9,36] Based on our findings of enhanced decidual senescence in *Ezh2*cKO stromal cells, we posit that impaired immune clearance of senescent stromal cells by uNK cells in *Ezh2*cKO uteri results in accumulation of senescent cells that contribute to defective decidualization.

Mechanistically, EZH2 downregulation induces cellular senescence by either methylation-independent activation of the DNA damage response or loss of methylation marks that result in elevation of the CDK inhibitors p21 and p16, critical for cell-cycle arrest and senescence.[45] Reduction in H3K27me3 levels and elevated p21 and p16 protein expression in stromal cells in *Ezh2*cKO uteri supports the hypothesis that *Ezh2* loss could reduce H3K27me3 levels and promote senescence through elevating p21 and p16. In human endometrial stromal cells, withdrawal of the decidualization stimulus resulted in dedifferentiation, disappearance of p53, and increased AKT activation.[46] Furthermore, loss of uterine p53 results in premature decidual senescence and promotes preterm birth through the COX2/PGF synthase pathway.[47] Decidual progression requires inactivation of AKT signaling in human endometrial stromal cells and increased activation compromises decidualization in patients with endometriosis.[48–50] We recently reported that *Ezh2*cKO mice show high estrogen-independent uterine *p*-AKT expression.[13] Our results also indicate that reduced p53 and elevated *p*-AKT expression in *Ezh2*-deleted stromal cells could be responsible for senescence-mediated defects during decidualization.

The placenta is critical for fetal growth and development and the majority of fetal growth restrictions result from abnormal placental development and function, which affects 3–8% of pregnancies worldwide.[51] As pregnancy progress, trophoblast cells directly interact with the decidualized stroma and its extracellular matrix (ECM) to form placenta.[52–54] Recent studies indicate that senescent human endometrial cells have degraded ECM compared to well-organized ECM in non-senescent cells. Inadequate interaction of trophoblastic cells with senescent endometrial cells could cause defective placentation in human.[29]

Increased senescence in decidua of *Ezh2*cKO mice may be positively correlated with the altered trophoblast differentiation. Some studies suggested that EZH2 expression is significantly decreased in placental villi of women who had recurrent miscarriages and its silencing in trophoblast cells attenuated trophoblast invasion.[55,56]

To further characterize uterine abnormalities affecting placenta development, we studied GD12 placentas in *Ezh2*cKO mice. Placentation defects included perturbations in trophoblast differentiation, size of the labyrinth and JZ, mislocalization of spongiotrophoblast cells, and reduced vascularization.[51] CDK p57 knockout mice have defective placenta development, leading to perinatal lethality.[30,31] Decreased p57 expression in *Ezh2*cKO mice indicated poor trophoblast differentiation in placenta. We found an attenuated labyrinth layer with aberrant infiltration of TPBPA-positive spongiotrophoblast cells and a less intricate vascular network, which caused placental insufficiency in *Ezh2*cKO mice. In addition to labyrinth defects, an extended JZ with reduced TPBPA-positive spongiotrophoblast cells indicated impaired placentation in these mice.

In summary, our results show that mice with a conditional uterine *Ezh2* deletion ovulate, and fertilization and embryo implantation subsequently occur normally. In contrast, infertility in *Ezh2*cKO mice is associated with defective decidualization and enhanced decidual senescence. Furthermore, these mice have altered trophoblast differentiation, resulting in placentation defects that culminate in mid-gestation pregnancy loss; these placental defects may be crucial for infertility in *Ezh2*cKO mice. Since the embryos in our studies were normal, the lack of *Ezh2* in the maternal uteri is the cause of pregnancy loss. This study provides important mechanistic insights to understand EZH2-mediated decidual senescence and unravel the role of maternal EZH2 loss in post-implantation placentation defects. Thus, our findings suggest that EZH2 loss or downregulation in pregnant women may cause increased miscarriages and infertility.

Limitations of the study

In this study, we show the impact of uterine EZH2 loss on pregnancy progression and its molecular mechanism in regulation of stromal cell decidualization and trophoblast differentiation in an *Ezh2*cKO mice model. However, there are some limitations of this study. We have utilized mouse models in this study and results must be validated in humans to correlate our findings for their clinical relevance. In addition, viable fetuses from *Ezh2*cKO dams need to be studied further to determine if there are any intrauterine growth restrictions and they are small for gestational age.

STAR★METHODS

Detailed methods are provided in the online version of this paper and include the following:

- KEY RESOURCES TABLE
- RESOURCE AVAILABILITY
  - Lead contact
  - Materials availability
  - Data and code availability
- EXPERIMENTAL MODEL AND STUDY PARTICIPANT DETAILS
  - *Generation of Ezh2*cKO *mice*
  - Artificial decidualization
- METHOD DETAILS
  - Fertility assessment, timed mating and tissue collection
  - Immunofluorescence
  - RNA isolation and RT-PCR
  - Immunohistochemistry
  - Mouse endometrial stromal cell (MESC) culture and *in vitro* decidualization
  - Senescence-associated β-galactosidase staining
  - Western blotting
- QUANTIFICATION AND STATISTICAL ANALYSIS

SUPPLEMENTAL INFORMATION

Supplemental information can be found online at https://doi.org/10.1016/j.isci.2023.107028.

ACKNOWLEDGMENTS

This work was supported by NIH grant R21HD088006 to PSC. Graphical abstract of this article was created with BioRender.com.

AUTHOR CONTRIBUTIONS

V.K.S., P.S.C., and I.C.B. designed the research; V.K.S., T.I.M., and A.K. performed the research; I.C.B. contributed new reagents/analytic tools; V.K.S., P.S.C., and I.C.B. analyzed the data; and V.K.S., P.S.C., and I.C.B. wrote the paper.

DECLARATION OF INTERESTS

The authors declare no competing interests.

Received: April 6, 2023
Revised: May 10, 2023
Accepted: May 30, 2023
Published: June 8, 2023

REFERENCES

1. Treviño, L.S., Wang, Q., and Walker, C.L. (2015). Phosphorylation of epigenetic "readers, writers and erasers": implications for developmental reprogramming and the epigenetic basis for health and disease. Prog. Biophys. Mol. Biol. *118*, 8–13. https://doi.org/10.1016/j.pbiomolbio.2015.02.013.

2. Jia, N., Li, Q., Tao, X., Wang, J., Hua, K., and Feng, W. (2014). Enhancer of zeste homolog 2 is involved in the proliferation of endometrial carcinoma. Oncol. Lett. *8*, 2049–2054. https://doi.org/10.3892/ol.2014.2437.

3. Oki, S., Sone, K., Oda, K., Hamamoto, R., Ikemura, M., Maeda, D., Takeuchi, M., Tanikawa, M., Mori-Uchino, M., Nagasaka, K., et al. (2017). Oncogenic histone methyltransferase EZH2: a novel prognostic marker with therapeutic potential in endometrial cancer. Oncotarget *8*, 40402–40411. https://doi.org/10.18632/oncotarget.16316.

4. Eskander, R.N., and Tewari, K.S. (2014). Exploiting the therapeutic potential of the PI3K-AKT-mTOR pathway in enriched populations of gynecologic malignancies. Expert Rev. Clin. Pharmacol. *7*, 847–858. https://doi.org/10.1586/17512433.2014.968554.

5. Yoo, K.H., and Hennighausen, L. (2012). EZH2 methyltransferase and H3K27 methylation in breast cancer. Int. J. Biol. Sci. *8*, 59–65. https://doi.org/10.7150/ijbs.8.59.

6. Bae, W.K., Yoo, K.H., Lee, J.S., Kim, Y., Chung, I.-J., Park, M.H., Yoon, J.H., Furth, P.A., and Hennighausen, L. (2015). The methyltransferase EZH2 is not required for mammary cancer development, although high EZH2 and low H3K27me3 correlate with poor prognosis of ER-positive breast cancers. Mol. Carcinog. *54*, 1172–1180. https://doi.org/10.1002/mc.22188.

7. Varambally, S., Dhanasekaran, S.M., Zhou, M., Barrette, T.R., Kumar-Sinha, C., Sanda, M.G., Ghosh, D., Pienta, K.J., Sewalt, R.G., Otte, A.P., et al. (2002). The polycomb group protein EZH2 is involved in progression of prostate cancer. Nature *419*, 624–629. https://doi.org/10.1038/nature01075.

8. Gan, L., Yang, Y., Li, Q., Feng, Y., Liu, T., and Guo, W. (2018). Epigenetic regulation of cancer progression by EZH2: from biological insights to therapeutic potential. Biomark. Res. *6*, 10. https://doi.org/10.1186/s40364-018-0122-2.

9. Fang, X., Ni, N., Lydon, J.P., Ivanov, I., Bayless, K.J., Rijnkels, M., and Li, Q. (2019). Enhancer of zeste 2 polycomb repressive complex 2 subunit is required for uterine epithelial integrity. Am. J. Pathol. *189*, 1212–1225. https://doi.org/10.1016/j.ajpath.2019.02.016.

10. Nanjappa, M.K., Mesa, A.M., Medrano, T.I., Jefferson, W.N., DeMayo, F.J., Williams, C.J., Lydon, J.P., Levin, E.R., and Cooke, P.S. (2019). The histone methyltransferase EZH2 is required for normal uterine development and function in mice. Biol. Reprod. *101*, 306–317. https://doi.org/10.1093/biolre/ioz097.

11. Mesa, A.M., Mao, J., Nanjappa, M.K., Medrano, T.I., Tevosian, S., Yu, F., Kinkade, J., Lyu, Z., Liu, Y., Joshi, T., et al. (2020). Mice lacking uterine enhancer of zeste homolog 2 have transcriptomic changes associated with uterine epithelial proliferation. Physiol. Genomics *52*, 81–95. https://doi.org/10.1152/physiolgenomics.00098.2019.

12. Mesa, A.M., Rosenfeld, C.S., Tuteja, G., Medrano, T.I., and Cooke, P.S. (2020). The roles of the histone protein modifier EZH2 in the uterus and placenta. Epigenomes *4*, 20. https://doi.org/10.3390/epigenomes4030020.

13. Sirohi, V.K., Medrano, T.I., Mesa, A.M., Kannan, A., Bagchi, I.C., and Cooke, P.S. (2022). Regulation of AKT signaling in mouse uterus. Endocrinology *163*, bqab233. https://doi.org/10.1210/endocr/bqab233.

14. Ramathal, C.Y., Bagchi, I.C., Taylor, R.N., and Bagchi, M.K. (2010). Endometrial decidualization: of mice and men. Semin. Reprod. Med. *28*, 17–26. https://doi.org/10.1055/s-0029-1242989.

15. Rubel, C.A., Jeong, J.-W., Tsai, S.Y., Lydon, J.P., and Demayo, F.J. (2010). Epithelial-stromal interaction and progesterone receptors in the mouse uterus. Semin. Reprod. Med. *28*, 27–35. https://doi.org/10.1055/s-0029-1242990.

16. Cha, J., Sun, X., and Dey, S.K. (2012). Mechanisms of implantation: strategies for successful pregnancy. Nat. Med. *18*, 1754–1767. https://doi.org/10.1038/nm.3012.

17. Pawar, S., Laws, M.J., Bagchi, I.C., and Bagchi, M.K. (2015). Uterine epithelial estrogen receptor-α controls decidualization via a paracrine mechanism. Mol. Endocrinol. *29*, 1362–1374. https://doi.org/10.1210/me.2015-1142.

18. Bhurke, A.S., Bagchi, I.C., and Bagchi, M.K. (2016). Progesterone-Regulated endometrial factors controlling implantation. Am. J. Reprod. Immunol. *75*, 237–245. https://doi.org/10.1111/aji.12473.

19. Bhurke, A., Kannan, A., Neff, A., Ma, Q., Laws, M.J., Taylor, R.N., Bagchi, M.K., and Bagchi, I.C. (2020). A hypoxia-induced Rab pathway regulates embryo implantation by controlled trafficking of secretory granules. Proc. Natl. Acad. Sci. USA *117*, 14532–14542. https://doi.org/10.1073/pnas.2000810117.

20. Davila, J., Laws, M.J., Kannan, A., Li, Q., Taylor, R.N., Bagchi, M.K., and Bagchi, I.C. (2015). Rac1 regulates endometrial secretory function to control placental development. PLoS Genet. *11*, e1005458. https://doi.org/10.1371/journal.pgen.1005458.

21. El Hachem, H., Crepaux, V., May-Panloup, P., Descamps, P., Legendre, G., and Bouet, P.-E. (2017). Recurrent pregnancy loss: current perspectives. Int. J. Womens Health *9*, 331–345. https://doi.org/10.2147/IJWH.S100817.

22. Garrido-Gomez, T., Dominguez, F., Quiñonero, A., Diaz-Gimeno, P., Kapidzic, M., Gormley, M., Ona, K., Padilla-Iserte, P., McMaster, M., Genbacev, O., et al. (2017). Defective decidualization during and after severe preeclampsia reveals a possible maternal contribution to the etiology. Proc. Natl. Acad. Sci. USA *114*, E8468–E8477. https://doi.org/10.1073/pnas.1706546114.

23. Kelleher, A.M., Milano-Foster, J., Behura, S.K., and Spencer, T.E. (2018). Uterine glands coordinate on-time embryo implantation and impact endometrial decidualization for pregnancy success. Nat. Commun. *9*, 2435. https://doi.org/10.1038/s41467-018-04848-8.

24. Salker, M., Teklenburg, G., Molokhia, M., Lavery, S., Trew, G., Aojanepong, T., Mardon, H.J., Lokugamage, A.U., Rai, R., Landles, C., et al. (2010). Natural selection of human embryos: impaired decidualization of endometrium disables embryo-maternal interactions and causes recurrent pregnancy loss. PLoS One *5*, e10287. https://doi.org/10.1371/journal.pone.0010287.

25. Grimaldi, G., Christian, M., Steel, J.H., Henriet, P., Poutanen, M., and Brosens, J.J. (2011). Down-regulation of the histone methyltransferase EZH2 contributes to the epigenetic programming of decidualizing human endometrial stromal cells. Mol. Endocrinol. *25*, 1892–1903. https://doi.org/10.1210/me.2011-1139.

26. Nancy, P., Siewiera, J., Rizzuto, G., Tagliani, E., Osokine, I., Manandhar, P., Dolgalev, I., Clementi, C., Tsirigos, A., and Erlebacher, A. (2018). H3K27me3 dynamics dictate evolving uterine states in pregnancy and parturition. J. Clin. Invest. *128*, 233–247. https://doi.org/10.1172/JCI95937.

27. Lucas, E.S., Dyer, N.P., Murakami, K., Lee, Y.H., Chan, Y.-W., Grimaldi, G., Muter, J., Brighton, P.J., Moore, J.D., Patel, G., et al. (2016). Loss of endometrial plasticity in recurrent pregnancy loss. Stem Cell. *34*, 346–356. https://doi.org/10.1002/stem.2222.

28. Lucas, E.S., Vrljicak, P., Muter, J., Diniz-da-Costa, M.M., Brighton, P.J., Kong, C.-S., Lipecki, J., Fishwick, K.J., Odendaal, J., Ewington, L.J., et al. (2020). Recurrent pregnancy loss is associated with a pro-senescent decidual response during the peri-implantation window. Commun. Biol. *3*, 37. https://doi.org/10.1038/s42003-020-0763-1.

29. Deryabin, P.I., and Borodkina, A.V. (2022). Stromal cell senescence contributes to impaired endometrial decidualization and defective interaction with trophoblast cells. Hum. Reprod. *37*, 1505–1524. https://doi.org/10.1093/humrep/deac112.

30. Zhang, P., Wong, C., DePinho, R.A., Harper, J.W., and Elledge, S.J. (1998). Cooperation between the *Cdk* inhibitors $p27^{KIP1}$ and $p57^{KIP2}$ in the control of tissue growth and development. Genes Dev. *12*, 3162–3167. https://doi.org/10.1101/gad.12.20.3162.

31. Takahashi, K., Kobayashi, T., and Kanayama, N. (2000). p57(Kip2) regulates the proper development of labyrinthine and spongiotrophoblasts. Mol. Hum. Reprod. *6*, 1019–1025. https://doi.org/10.1093/molehr/6.11.1019.

32. Rai, R., and Regan, L. (2006). Recurrent miscarriage. Lancet *368*, 601–611. https://doi.org/10.1016/S0140-6736(06)69204-0.

33. Quenby, S., Gallos, I.D., Dhillon-Smith, R.K., Podesek, M., Stephenson, M.D., Fisher, J., Brosens, J.J., Brewin, J., Ramhorst, R., Lucas, E.S., et al. (2021). Miscarriage matters: the epidemiological, physical, psychological, and economic costs of early pregnancy loss. Lancet *397*, 1658–1667. https://doi.org/10.1016/S0140-6736(21)00682-6.

34. Ni, N., Jalufka, F.L., Fang, X., McCreedy, D.A., and Li, Q. (2022). Role of EZH2 in uterine gland development. Int. J. Mol. Sci. *23*, 15665. https://doi.org/10.3390/ijms232415665.

35. Du, L., Deng, W., Zeng, S., Xu, P., Huang, L., Liang, Y., Wang, Y., Xu, H., Tang, J., Bi, S., et al. (2021). Single-cell transcriptome analysis reveals defective decidua stromal niche attributes to recurrent spontaneous abortion. Cell Prolif. *54*, e13125. https://doi.org/10.1111/cpr.13125.

36. Osokine, I., Siewiera, J., Rideaux, D., Ma, S., Tsukui, T., and Erlebacher, A. (2022). Gene silencing by EZH2 suppresses TGF-β activity within the decidua to avert pregnancy-adverse wound healing at the maternal-fetal interface. Cell Rep. *38*, 110329. https://doi.org/10.1016/j.celrep.2022.110329.

37. Alam, S.M.K., Konno, T., and Soares, M.J. (2015). Identification of target genes for a prolactin family paralog in mouse decidua. Reproduction *149*, 625–632. https://doi.org/10.1530/REP-15-0107.

38. Alam, S.M.K., Konno, T., Dai, G., Lu, L., Wang, D., Dunmore, J.H., Godwin, A.R., and Soares, M.J. (2007). A uterine decidual cell cytokine ensures pregnancy-dependent adaptations to a physiological stressor. Development *134*, 407–415. https://doi.org/10.1242/dev.02743.

39. Li, Q., Kannan, A., Wang, W., DeMayo, F.J., Taylor, R.N., Bagchi, M.K., and Bagchi, I.C. (2007). Bone morphogenetic protein 2 functions via a conserved signaling pathway involving wnt4 to regulate uterine decidualization in the mouse and the human. J. Biol. Chem. *282*, 31725–31732. https://doi.org/10.1074/jbc.M704723200.

40. He, S., and Sharpless, N.E. (2017). Senescence in health and disease. Cell *169*, 1000–1011. https://doi.org/10.1016/j.cell.2017.05.015.

41. Tomari, H., Kawamura, T., Asanoma, K., Egashira, K., Kawamura, K., Honjo, K., Nagata, Y., and Kato, K. (2020). Contribution of senescence in human endometrial stromal cells during proliferative phase to embryo receptivity. Biol. Reprod. *103*, 104–113. https://doi.org/10.1093/biolre/ioaa044.

42. Rawlings, T.M., Makwana, K., Taylor, D.M., Molè, M.A., Fishwick, K.J., Tryfonos, M., Odendaal, J., Hawkes, A., Zernicka-Goetz, M., Hartshorne, G.M., et al. (2021). Modelling the impact of decidual senescence on embryo implantation in human endometrial assembloids. Elife *10*, e69603. https://doi.org/10.7554/eLife.69603.

43. Brighton, P.J., Maruyama, Y., Fishwick, K., Vrljicak, P., Tewary, S., Fujihara, R., Muter, J., Lucas, E.S., Yamada, T., Woods, L., et al. (2017). Clearance of senescent decidual cells by uterine natural killer cells in cycling human endometrium. Elife *6*, e31274. https://doi.org/10.7554/eLife.31274.

44. Deryabin, P., Griukova, A., Nikolsky, N., and Borodkina, A. (2020). The link between endometrial stromal cell senescence and decidualization in female fertility: the art of balance. Cell. Mol. Life Sci. *77*, 1357–1370. https://doi.org/10.1007/s00018-019-03374-0.

45. Ito, T., Teo, Y.V., Evans, S.A., Neretti, N., and Sedivy, J.M. (2018). Regulation of cellular senescence by polycomb chromatin modifiers through distinct DNA damage- and histone methylation-dependent pathways. Cell Rep. *22*, 3480–3492. https://doi.org/10.1016/j.celrep.2018.03.002.

46. Pohnke, Y., Schneider-Merck, T., Fahnenstich, J., Kempf, R., Christian, M., Milde-Langosch, K., Brosens, J.J., and Gellersen, B. (2004). Wild-type p53 protein is up-regulated upon cyclic adenosine monophosphate-induced differentiation of human endometrial stromal cells. J. Clin. Endocrinol. Metab. *89*, 5233–5244. https://doi.org/10.1210/jc.2004-0012.

47. Hirota, Y., Daikoku, T., Tranguch, S., Xie, H., Bradshaw, H.B., and Dey, S.K. (2010). Uterine-specific p53 deficiency confers premature uterine senescence and promotes preterm birth in mice. J. Clin. Invest. *120*, 803–815. https://doi.org/10.1172/JCI40051.

48. Yoshino, O., Osuga, Y., Hirota, Y., Koga, K., Yano, T., Tsutsumi, O., and Taketani, Y. (2003). Akt as a possible intracellular mediator for decidualization in human endometrial stromal cells. Mol. Hum. Reprod. *9*, 265–269. https://doi.org/10.1093/molehr/gag035.

49. Yin, X., Pavone, M.E., Lu, Z., Wei, J., and Kim, J.J. (2012). Increased activation of the PI3K/AKT pathway compromises decidualization of stromal cells from endometriosis. J. Clin. Endocrinol. Metab. *97*, E35–E43. https://doi.org/10.1210/jc.2011-1527.

50. Fabi, F., Grenier, K., Parent, S., Adam, P., Tardif, L., Leblanc, V., and Asselin, E. (2017). Regulation of the PI3K/Akt pathway during decidualization of endometrial stromal cells. PLoS One *12*, e0177387. https://doi.org/10.1371/journal.pone.0177387.

51. Woods, L., Perez-Garcia, V., and Hemberger, M. (2018). Regulation of placental development and its impact on fetal growth—new insights from mouse models. Front. Endocrinol. *9*, 570. https://doi.org/10.3389/fendo.2018.00570.

52. Laguë, M.N., Detmar, J., Paquet, M., Boyer, A., Richards, J.S., Adamson, S.L., and Boerboom, D. (2010). Decidual PTEN expression is required for trophoblast invasion in the mouse. Am. J. Physiol. Endocrinol. Metab. *299*, E936–E946. https://doi.org/10.1152/ajpendo.00255.2010.

53. Peng, J., Monsivais, D., You, R., Zhong, H., Pangas, S.A., and Matzuk, M.M. (2015). Uterine activin receptor-like kinase 5 is crucial for blastocyst implantation and placental development. Proc. Natl. Acad. Sci. USA *112*, E5098–E5107. https://doi.org/10.1073/pnas.1514498112.

54. Xiao, Z., Yan, L., Liang, X., and Wang, H. (2020). Progress in deciphering trophoblast cell differentiation during human placentation. Curr. Opin. Cell Biol. *67*, 86–91. https://doi.org/10.1016/j.ceb.2020.08.010.

55. Lv, S., Wang, N., Lv, H., Yang, J., Liu, J., Li, W.-P., Zhang, C., and Chen, Z.-J. (2019). The attenuation of trophoblast invasion caused by the downregulation of EZH2 is involved in the pathogenesis of human recurrent miscarriage. Mol. Ther. Nucleic Acids *14*, 377–387. https://doi.org/10.1016/j.omtn.2018.12.011.

56. Shang, Y., Wu, S., Li, S., Qin, X., Chen, J., Ding, J., and Yang, J. (2022). Downregulation of EZH2 in trophoblasts induces decidual m1 macrophage polarization: a potential cause of recurrent spontaneous abortion. Reprod. Sci. *29*, 2820–2828. https://doi.org/10.1007/s43032-021-00790-1.

STAR★METHODS

KEY RESOURCES TABLE

REAGENT or RESOURCE	SOURCE	IDENTIFIER
Antibodies		
Rabbit monoclonal anti-MKI67	Abcam	Cat# ab16667; RRID: AB_302459
Rat monoclonal anti-KRT8	Developmental Studies Hybridoma Bank	Cat# TROMA-I; RRID: AB_531826
Rabbit polyclonal anti-CD31	Abcam	Cat# ab124432; RRID: AB_2802125
Mouse monoclonal anti-p21	Santa Cruz Biotechnology	Cat# sc-6246; RRID: AB_628073
Rabbit monoclonal anti-p16	Cell Signaling Technology	Cat# 80772; RRID: AB_2799960
Mouse monoclonal anti-p53	Cell Signaling Technology	Cat# 2524; RRID: AB_331743
Mouse monoclonal anti-GAPDH	Proteintech	Cat# 60004-1-Ig; RRID: AB_2107436
Rabbit monoclonal anti-H3K27me3	Cell Signaling Technology	Cat# 9733; RRID: AB_2616029
Mouse monoclonal anti-H3	Cell Signaling Technology	Cat# 14269; RRID: AB_2756816
Rabbit monoclonal anti *p*-AKT	Cell Signaling Technology	Cat# 4060; RRID: AB_2315049
Rabbit monoclonal anti-AKT	Cell Signaling Technology	Cat# 4685; RRID: AB_2225340
Rabbit polyclonal anti-TPBPA	Abcam	Cat# ab104401; RRID: AB_10901888
Rabbit polyclonal anti-p57	Santa Cruz Biotechnology	Cat# sc-8298; RRID: AB_2078155
Goat Anti-Mouse IgG (H + L)-HRP Conjugate	Bio-Rad	Cat# 1706516; RRID: AB_11125547
Goat Anti-Rabbit IgG (H + L)-HRP Conjugate	Bio-Rad	Cat# 1706515; RRID: AB_11125142
Alexa Fluor® 488 AffiniPure Donkey Anti-Rabbit IgG	Jackson ImmunoResearch Labs	Cat# 711-545-152; RRID: AB_2313584
Alexa Fluor® 488 AffiniPure Donkey Anti-Rat IgG	Jackson ImmunoResearch Labs	Cat# 712-545-150; RRID: AB_2340683
Rhodamine (TRITC) AffiniPure Donkey Anti-Rat IgG	Jackson ImmunoResearch Labs	Cat# 712-025-153; RRID: AB_2340636
Chemicals, peptides, and recombinant proteins		
Estradiol	Sigma-Aldrich	Cat# E1024
Progesterone	Sigma-Aldrich	Cat# P0130
Dimethyl sulfoxide	Sigma-Aldrich	Cat# D4540
Hydrogen Peroxide, 30%	Fisher Scientific	Cat# H325-500
Methanol	Fisher Scientific	Cat# A452-4
Hematoxylin Solution, Gill No. 2	Sigma-Aldrich	Cat# GHS216
Sodium Dodecyl Sulfate	Fisher Scientific	Cat# BP166
SuperSignal™ West Pico PLUS Chemiluminescent Substrate	Thermo Fisher Scientific	Cat# 34577
Corn oil	Sigma-Aldrich	Cat# C8267
Normal Goat Serum Blocking Solution	Vector Laboratories	Cat# S-1000
Hank's Balanced Salt Solution	CORNING Life Sciences	Cat# 20-021-CVR
DMEM/Hams F-12 50/50 Mix	CORNING Life Sciences	Cat# 10-090-CV
Fetal Bovine Serum, charcoal stripped	Gibco	Cat# A3382101
DAPI	Electron Microscopy Sciences	Cat# 17984-24
Sodium Citrate Dihydrate	Fisher Scientific	Cat# BP327
0.25% Trypsin-EDTA	CORNING Life Sciences	Cat# 25-053
Antibiotic-Antimycotic	Gibco	Cat# 15240062
Halt™ Protease Inhibitor Cocktail (100X)	Thermo Scientific™	Cat# 87786
TRIzol™ Reagent	Invitrogen™	Cat# 15596026

(*Continued on next page*)

Continued

REAGENT or RESOURCE	SOURCE	IDENTIFIER
Collagenase	Sigma-Aldrich	Cat# C2674
Pancreatin	Sigma-Aldrich	Cat# P3292
Dispase	Sigma-Aldrich	Cat# D4693
2-Mercaptoethanol	Bio-Rad	Cat# 1610710
Neutral buffered formalin	Fisher Scientific	Cat# SF100
Critical commercial assays		
Vectastain® Elite ABC-HRP Kit	Vector Laboratories	Cat# PK-4000; RRID: AB_2336820
PrimeScript™ RT reagent kit	Takara Bio	Cat #RR037A
PrimeScript™ perfect real-time TB green	Takara Bio	Cat# RR0420A
DAB Substrate Kit (3,3′-diaminobenzidine)	Vector Laboratories	Cat# SK-4100; RRID: AB_2336382
Senescence-associated β-galactosidase staining kit	Cell Signaling Technology	Cat# 9860
Pierce™ BCA protein assay kit	Thermo Scientific™	Cat# 23250
Experimental models: Organisms/strains		
$Ezh2^{flox/flox}$ mice	Jackson Laboratories	Stock # 022616
$Pgr^{wt/Cre}$ mice	Gift of Drs, John Lydon (Baylor College of Medicine, Houston TX) and Franco DeMayo (NIEHS, Research Triangle Park NC)	N/A
Oligonucleotides		
Full list of qRT-PCR primers, see Tables S1 and S2	This paper	N/A
Software and algorithms		
ImageJ	National Institutes of Health	https://imagej.nih.gov/ij/
GraphPad Prism	GraphPad Software	www.graphpad.com

RESOURCE AVAILABILITY

Lead contact

Further information and requests for resources and reagents should be directed to and will be fulfilled by the lead contact, Paul S. Cooke (Paulscooke@ufl.edu).

Materials availability

This study did not generate new unique reagents.

Data and code availability

- All data reported in this paper will be shared by the lead contact upon request.
- This study did not generate original code.
- Any additional information required to reanalyze the data reported in this paper is available from the lead contact upon request.

EXPERIMENTAL MODEL AND STUDY PARTICIPANT DETAILS

Generation of Ezh2cKO mice

Adult female *Ezh2*cKO mice with a conditional deletion of uterine *Ezh2* were generated using mice that were homozygous for floxed *Ezh2* and also expressed Cre recombinase driven by the progesterone receptor gene. Mice were housed in standard polycarbonate/polysulfone cages at 25°C with 12L:12D cycles and given water and a standard rodent diet *ad libitum*. All animal experiments were approved by the IACUC of the University of Florida and conducted in accordance with the NIH Guide for the Care and Use of Laboratory Animals. Genotyping of transgenic mice was performed by multiplex PCR on genomic DNA (Table S1).

Artificial decidualization

Uterine stromal decidualization was experimentally induced in adult ovariectomized hormone-primed mice as described previously.[19] Briefly, adult female WT and *Ezh2*cKO mice were ovariectomized. Two weeks later, mice were injected with 100 ng of 17β-estradiol (E2) in 0.1 mL of corn oil subcutaneously (sc) every 24 h for three consecutive days. After two days of rest, sc hormone injections containing 1 mg progesterone (P4) and 10 ng E2 in 0.1 mL vehicle were given daily for three consecutive days. Decidualization was induced in one horn by injecting 20 μL of oil into the lumen, while the other horn was left unstimulated as an internal control. Mice were treated with additional daily E2 + P4 injections for up to 96 h post-stimulus. Mice were euthanized, uterine horns were collected and each uterine horn was weighed separately. Unstimulated and stimulated uterine horns were fixed in formalin and processed for histology.

METHOD DETAILS

Fertility assessment, timed mating and tissue collection

Fertility of *Ezh2*cKO mice was assessed up to 8–9 months of age, as we have described previously.[10] Pup number in the first litter was also counted. For timed mating experiments, WT and *Ezh2*cKO mice were mated with fertile wild-type males. Gestation day (GD) 1 was defined as the day the vaginal plug was observed. To examine implantation sites throughout gestation, pregnant mice were sacrificed on the morning of GD7, 10, 12 and 15. Number and diameter of implantation sites were recorded using Vernier calipers. Implantation sites were collected in 10% neutral buffered formalin and paraffin embedded for immunohistochemistry and immunofluorescence. For RNA experiments, embryos were removed from implantation sites using fine forceps and uteri were frozen at −80°C until further processing.

Immunofluorescence

Uterine tissues were processed and subjected to immunofluorescence as described previously.[20] Briefly, paraffin-embedded tissues were sectioned at 5 μm and mounted on microscopic slides. Sections were deparaffinized in xylene, rehydrated through a series of ethanol washes, and rinsed in water. Antigen retrieval was performed by immersing the slides in 0.1M citrate buffer solution, pH 6.0, followed by microwave heating for 25 min. The slides were allowed to cool and endogenous peroxidase activity was blocked by incubating sections in 0.3% hydrogen peroxide in methanol for 15 min at room temperature. After washing with PBS for 15 min, the slides were incubated in a goat serum blocking solution for 1 h. This was followed by incubation overnight at 4°C with antibodies specific for cytokeratin 8 (KRT8, 1:50, Developmental Studies Hybridoma Bank, TROMA-1), platelet/endothelial cell adhesion molecule 1 (PECAM1/CD31, 1:250, Abcam), and MKI67 (1:500, Abcam).

Placental sections were also subjected to immunofluorescence using these primary antibodies: cytokeratin 8, PECAM1/CD31, trophoblast specific protein alpha, (1:500, Abcam), and p57 (1:100, Santa Cruz Biotechnology). Secondary antibodies including fluorescent-tagged rhodamine donkey anti-rabbit, 488 donkey anti-mouse, 488 donkey anti-rabbit, 488 donkey anti-goat were purchased from Jackson Immuno Research. Fluoromount-G with DAPI was from eBiosciences. Images were captured using the Olympus BX51 microscope equipped for fluorescence and connected to a Jenoptik ProgRes C14 digital camera with c-mount interface containing a 1.4 Megapixel CCD sensor. Fluorescent images were processed and merged using Adobe Photoshop Extended CS6 (Adobe Systems).

RNA isolation and RT-PCR

Total RNA was isolated from uterine tissues and cultured mouse endometrial stromal cells (MESCs) using TRIzol as per the manufacturer's protocol. Total RNA concentration was determined using a NanoDrop-200 spectrophotometer (Thermo). RNA was transcribed to cDNA using the PrimeScript RT reagent kit (Takara Bio #RR037A). For mRNA expression, PrimeScript perfect real-time TB green (Takara Bio #RR0420A) was used and amplification was performed in a CFX96 thermal cycler (Bio-Rad). Threshold cycle values (CT) were exported as an excel file and the ΔΔCt method was utilized for relative RNA expression analysis. Target gene expression was normalized against a housekeeping gene, *Rplp0*. Experiments were performed in triplicate with three different animals or cell cultures in each set. Graphs were plotted as mean fold-change +SEM relative to WT control. Primer sequences are listed in Table S2.

Immunohistochemistry

Sections (5–6 μm) of paraffin-embedded implantation sites were cut with a microtome. Immunohistochemistry was performed using the Vectastain Elite ABC-HRP Kit (Vector Laboratories), with minor modifications. Uterine sections were deparaffinized and rehydrated. Antigen retrieval was performed in boiling sodium citrate buffer and endogenous peroxidase activity was blocked using hydrogen peroxide, as described.[13] Slides were incubated with primary antibody against MKI67 (Abcam, dilution 1:500) at 4°C overnight. The chromogen substrate 3, 3′-diaminobenzidine (DAB; Vector Laboratories, Burlingame, CA) was used to detect positively stained cells. Slides were counterstained using Gill hematoxylin (Sigma-Aldrich) for 15 s and mounted with Permount (Fisher Scientific). Images were captured using an Olympus BH-2 microscope under bright field illumination with a 25X lens.

Mouse endometrial stromal cell (MESC) culture and *in vitro* decidualization

The MESCs were isolated from GD4 uteri, as previously described.[19] In brief, uteri from *Ezh2*cKO and WT mice cleaned of fat were washed and cut open longitudinally, and digested by incubating with 6 mg/mL dispase (Sigma, D4693) and 25 mg/mL pancreatin (Sigma, P3292) in a 1x Hanks Balanced Salt Solution (HBSS) for 45 min at room temperature, followed by 15 min at 37°C. Following incubation, supernatant containing epithelial cells was removed by aspiration and the enzymatic reaction was stopped by adding heat-inactivated fetal bovine serum (FBS) to remaining tissue pieces. Uterine fragments were washed twice with HBSS to remove the serum. Uterine fragments were digested in 5 mL HBSS solution containing 0.15 g/L collagenase for 1 h at 37°C in a shaker incubator. After digestion, 10% FBS in 5 mL of HBSS was added to stop enzymatic digestion. Endometrial stromal cells were separated as described previously[19] and resuspended in DMEM/F12 supplemented with an antibiotic and antimycotic solution, 2% (v/v) charcoal stripped FBS, 10 nM E2 and 1 μM P4. The MESC were seeded in T-25 culture flasks at an initial plating density of 4×10^5 cells. After 72 h incubation in E2-and P4-supplemented DMEM/F12, cells were detached from the flasks and lysed either in SDS buffer for western blotting or in Trizol for RNA extraction. Three independent replicates derived from WT or *Ezh2*cKO uteri were utilized for each group.

Senescence-associated β-galactosidase staining

Senescence-associated β-galactosidase (SA-β-Gal) staining was performed using the senescence β-galactosidase staining kit (Cell Signaling Technology #9860) according to manufacturer's instructions. In brief, MESCs were seeded in 6-well plate and decidualized for 72h as described above. Following treatment, cells were washed with PBS, placed in the fixative provided for 10 min and then washed twice with PBS. Fixed cells were then incubated in a staining solution (pH 6) in a 37°C incubator without CO_2 for at least 16h. Images of random fields were captured using bright-field phase contrast microscopy.

Western blotting

The MESCs were lysed, homogenized in 1% SDS lysis buffer supplemented with Halt protease inhibitor cocktail (Thermo Scientific) and kept for 10 min at 95°C. Lysates were centrifuged at 1800 x g for 5 min to remove cell debris. Protein content of the lysate was estimated using the Pierce BCA protein assay kit (ThermoFisher Scientific). Equal amounts of protein lysates were separated by SDS-PAGE gel electrophoresis (Bio-Rad) and transferred to Immobilon-P PVDF membrane (Millipore). Non-specific binding was blocked using 5% nonfat dry milk for 1 h at room temperature and then the membrane was incubated with a primary antibody against p21 (Santa Cruz Biotechnology sc-6246, 1:250), p16 (Cell Signaling Technology #80772, 1:1000), p53 (Cell Signaling Technology #2524, 1:1000), H3K27me3 (Cell Signaling Technology #9733, 1:1000) *p*-AKT or AKT (Cell Signaling Technology #4060, 1:2000 or #4685, 1:1000, respectively) or GAPDH (Proteintech 60004-1-Ig, 1:5000) at 4°C overnight. The next day, membranes were washed with TBS-T and incubated with horseradish peroxidase-conjugated secondary antibody for 1h. Antibody binding was visualized with SuperSignal west pico PLUS chemiluminescent substrate (Thermo Scientific) and images were captured by C-DiGit blot scanner (LI-COR Biosciences). Band intensities were quantified with ImageJ software.

QUANTIFICATION AND STATISTICAL ANALYSIS

Data are presented as mean ± SEM and were analyzed using the Student's *t* test. Differences between groups were considered significant at $p < 0.05$. Statistical analysis was performed using Graph Pad Prism 9.0 (Graph Pad Software, Inc., San Diego, CA).